ON THE STRETCHING OF MESOSCALE VORTICES INTO FILAMENTS AND THEIR DISTRIBUTION OVER THE OCEAN SURFACE

V. V. Zhmur,[1,2,3*] **T. V. Belonenko,**[3]
E. V. Novoselova,[3] **and B. S. Suetin**[2]   UDC 551.465

We consider various aspects of interaction of vortices with a barotropic flow. When a vortex interacts with a flow, there exist three variants of the flow-core behavior: rotation, nutational oscillations, and unlimited stretching. In the first two cases, the vortex remains a localized formation, such that the ellipse semiaxes undergo oscillations near certain average values. In the third case, the shape of the vortex varies as follows: one horizontal axis increases indefinitely and the second horizontal axis tends to zero so that the vertical size of the vortex does not change and the vortex itself stretches into a filament in top view, remaining ellipsoidal. As a result, vortex formations, which are called filaments, emerge in the ocean. They emerge from the vortices which are initially almost circular in the horizontal plane and represent structures stretched in one direction and having nonzero vorticity. In this work, an analytical and graphical method for determining the regimes of behavior of three-dimensional ellipsoidal vortices is proposed for the first time for an inhomogeneous horizontal current which is linear with respect to the horizontal coordinates. Conditions for inevitable stretching of the vortices into filaments are studied. It is established that the vortex stretching is manifested in spots (domains) on 60–67% of the world ocean surface and the characteristic dimensions of these spots amount to about 200 km. The vortex stretching into filaments ensures energy pumping from mesoscale processes to submesoscale ones. According to the global oceanic reanalysis GLORYS12V1, the domain distributions in the World Ocean are plotted. It is shown that irrespective of the spatial-averaging scales, the integral area of regions in which the mesoscale vortices can stretch into filaments is dominant.

1. INTRODUCTION

In 1978, the USSR Committee for Inventions registered the discovery of the existence of synoptic (mesoscale) vortices in the ocean. This discovery was the result of fundamental research on measuring currents, which was carried out for seven months during the implementation of the "POLYGON-70" program in the North Atlantic tropical zone in 1970. Further studies of mesoscale vortices in the ocean were continued during the Soviet-American experiments under the program MODE (Sargasso Sea, 1973), POLY-MODE (North Atlantic, 1977-1978), MESOPOLYGON (North Atlantic, 1985), and MEGAPOLYGON (Pacific Ocean, 1987). The experiments raised a number of important issues concerning the physics of the ocean vortices [1].

Today, the future of modern oceanology is impossible to imagine without the use of the satellite methods for obtaining information about the ocean, which is due to their main undeniable advantages such

---

* zhmur-vladimir@mail.ru

1

as spatial representativeness ensuring regional and global research, efficiency of obtaining information, the ability to arrange operational integrated monitoring anywhere in the World Ocean, and low cost of satellite monitoring compared with the contact ocean-exploration methods [2]. Progress in the remote sensing of the Earth and the development of altimetric methods for studying the ocean allow one to currently carry out daily monitoring of the sea surface on a regular basis and obtain an up-to-date information on the surface of the World Ocean, and analyze the variability of mesoscale vortices and currents [3, 4]. With the development of computer technologies and hydrodynamic models, it became possible to use simulation data for the study of currents and vortices, including reanalysis, in which the hydrodynamic model assimilates the satellite and *in situ* measurements, as well as the data from drifters, Argo buoys, and gliders.

The study of mesoscale vortices gives knowledge about various systems of interconnected oceanic characteristics and is one of the most important tasks of the ocean hydromechanics. The mesoscale vortices have their own dynamics with dominating nonlinear effects. Such vortices are formed almost everywhere in the entire water area of the World Ocean [5] and capable of transferring heat, mass, kinetic energy, and biochemical characteristics from the region of their formation over very long distances, which affects climatic fluctuations. Despite significant progress in studying the kinematic properties and dynamic features of vortices, their nature still needs to be studied. This refers, in particular, to the behavior of the cores of the vortices, their interaction with each other and with currents, as well as the survival of the vortices in the inhomogeneous external currents.

In 1948, S. A. Chaplygin published work [6] in which the strain of a two-dimensional Kirchhoff vortex by a constant-shear flow was considered. These studies were continued by S. Kida [7]. For three-dimensional vortices, this concept is extended in [8–14], where the theory of evolution of ellipsoidal vortices in the ocean under the action of currents was developed. The conclusions of this theory are as follows: when a vortex interacts with a current, there exist three variants of the vortex behavior, namely, rotation, nutational oscillations, and unlimited stretching. In the first two cases, the vortex remains a localized formation, and although the semiaxes of the ellipse undergo oscillations near certain average values, they still remain limited, as the vortex itself. In the third case, the shape of the vortex changes as follows: one of the horizontal axes increases indefinitely, the second horizontal axis tends to zero, while preserving the vertical size, and the vortex itself stretches into a filament, in the horizontal plane still remaining ellipsoidal. As a result, when viewed from above, the vortex filaments are formed in the ocean. They emerge from the initially circular vortices in the horizontal plane and represent structures elongated in one direction with nonzero vorticity. The satellite shot (Fig. 1) clearly shows the vortex filaments on the sea surface. Note that such a pattern is typical of many radar images.

This work is aimed at studying the evolution of the mesoscale vortices when they are stretched to form filaments on the basis of the theory and the reanalysis data.

2. THEORETICAL BACKGROUND

Let us briefly discuss the main events, which are observed during the vortex interaction with a current.

For the barotropic currents $\mathbf{u} = (u, v, 0)$ with the most general linear dependence of the current velocity on the horizontal coordinates in the form

$$\mathbf{u} = (u, v, 0) = \begin{cases} u = u_0 + ex - \gamma y; \\ v = v_0 + \gamma x - ey \end{cases}, \tag{1}$$

the problem of the vortex interaction with a current is reduced to determining the time evolution of two horizontal ellipsoid semiaxes $a(t)$ and $b(t)$ (it is assumed for definiteness that a and b are the major and minor semiaxes, respectively). Here, x and y are the horizontal coordinates, z is the vertical coordinate with the axis directed upwards, and u_0 and v_0 are the components of the current velocity at the vortex center with $x = 0$ and $y = 0$. The coefficients γ and e describe the spatial variability of the background current, such that $\gamma = (1/2)|\text{rot}_z \mathbf{u}|$ is the angular velocity of rotation of liquid particles in the background current and e is the strain coefficient of the background current. The coordinate system of (x, y, z) for Eqs. (1) is chosen

2

65.94° N
37.22° E

65.66° N
39.69° E

65.18° N
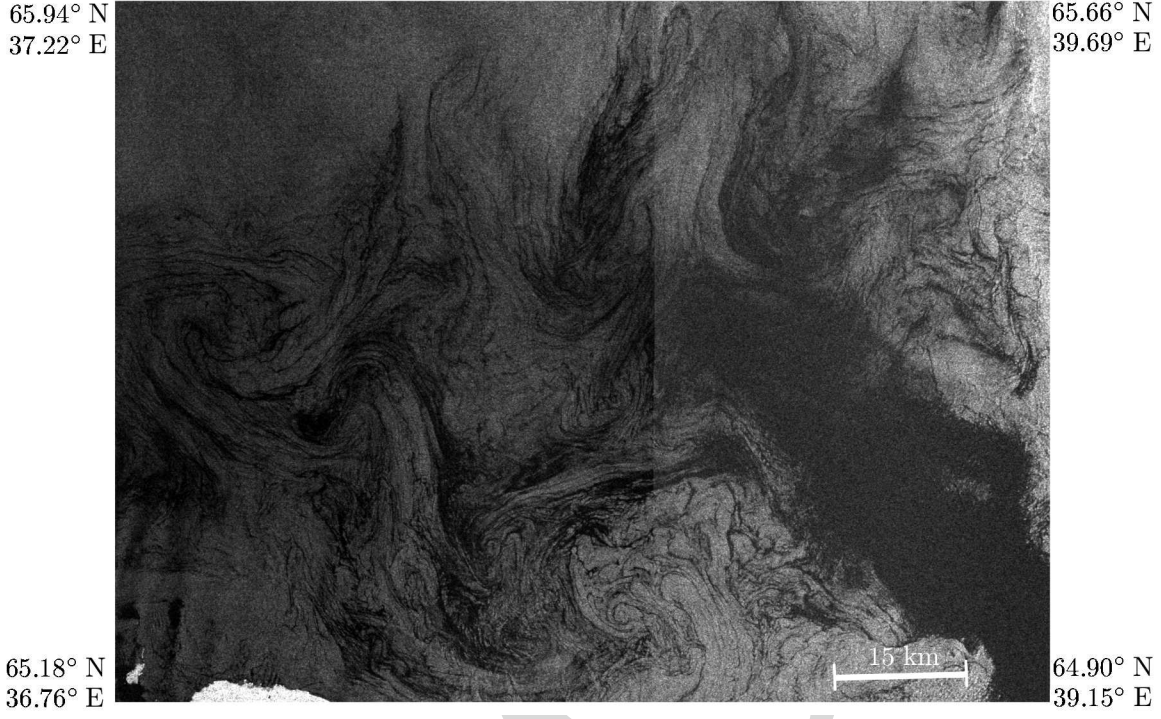36.76° E

15 km

64.90° N
39.15° E

Fig. 1. Examples of manifestations of the filaments in the White Sea in the Envisat ASAR radar image at 08:11 UTC of 2010 (the data from the European Space Agency).

such that the coefficient $(-\gamma)$ of the coordinate y in the x component of the velocity and the coefficient γ of the coordinate x in the y component of the velocity are identical in magnitude, but have opposite signs. In addition, the divergenceless of the current (1) yields $e = \partial u/\partial x = -(\partial v/\partial y)$. Such a coordinate system can always be obtained from any other coordinate system with the vertical axis z in the case of an arbitrary linear dependence of the velocity vector of the barotropic current on the horizontal coordinates by rotating the coordinate system around the vertical axis z. It is exactly this "convenient" coordinate system that is used in [7] when studying the evolution of the Kirchhoff vortex in the current. In a barotropic current, the vortex center moves as a whole body with a velocity of the external current falling at the ellipsoid center. The vertical semiaxis c is constant, while the horizontal axes vary such that the product $a(t)b(t)$ is preserved [8].

Thus, the main variables characterizing the problem are γ, e, and σ and having the dimension c^{-1}, and σ is the redundant potential vorticity of the vortex core above the potential vorticity 2γ of the background current (1) [15–17]. The problem of evolution of the vortex shape can be reduced to a system of two differential equations for the ratio $\varepsilon = a/b$ of the semiaxes and the orientation angle θ between the major horizontal semiaxis a of the ellipsoid and the coordinate axis x [8, 14]:

$$\dot{\varepsilon} = 2\varepsilon e \cos(2\theta), \tag{2}$$

$$\dot{\theta} = \Omega(\varepsilon, K) + \gamma - \frac{\varepsilon^2 + 1}{\varepsilon^2 - 1} e \sin(2\theta). \tag{3}$$

Here, $K = (N/f)\,(c/\sqrt{ab})$ is the parameter of the vertical oblation of the core, where N is the Brunt–Väisälä frequency, f is the Coriolis parameter, and

$$\Omega(\varepsilon, K) = \frac{1}{2}\sigma K \int\limits_0^\infty \frac{\mu\,\mathrm{d}\mu}{\sqrt{(\mu + \varepsilon)\,(\mu + 1/\varepsilon)\,(K^2 + \mu)}}. \tag{4}$$

In the general case, $\Omega(\varepsilon, K)$ is the variable natural angular velocity of the core-shape rotation (not to be confused with the angular velocity of rotation of particles in the core), which depends on ε, K, and σ. The
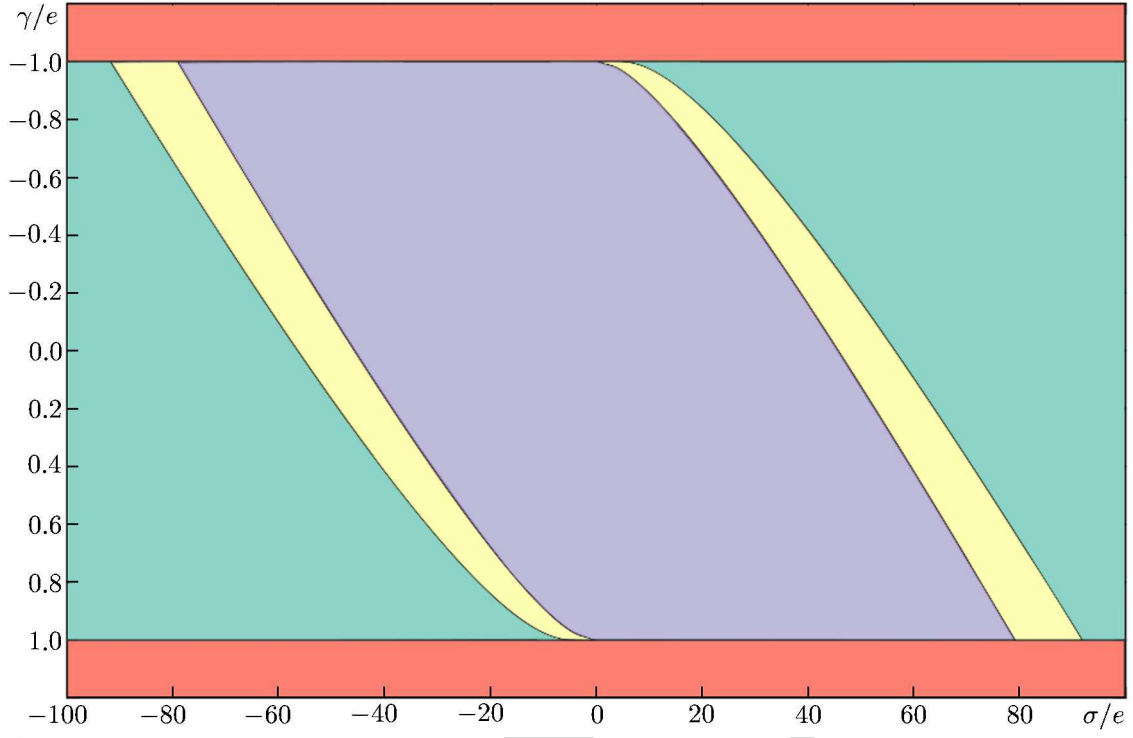
3

Fig. 2. Diagram of the zones of different behavior of the vortices in the case $K = 0.2$ in the parameter plane. $(\sigma/e, \gamma/e)$

details of deriving Eqs. (2) and (3) and the simplest properties of the vortex-core evolution are given in the Appendix (see [8, 14]) and their further development, in [18–20].

Equations (2)–(4) describe the evolution of the core shape, which occurs because of the spatial inhomogeneity of the background current characterized by the strain coefficient e. In the case of constant coefficients e and γ, the system is solved in quadratures:

$$\sin(2\theta) = \frac{\varepsilon}{\varepsilon^2 - 1} C + \frac{\varepsilon}{\varepsilon^2 - 1} \int\limits_1^\varepsilon \frac{\mu^2 - 1}{\mu^2} \frac{\Omega(\mu, K) + \gamma}{e} \, d\mu, \tag{5}$$

where C is an arbitrary integration constant. Any integral curve in the parameter plane $(\varepsilon, \sin(2\theta))$ describes the evolution of a particular vortex, which depends on the parameters e and γ of the background current, the parameter K of the vertical oblation of the vortex core, and the value of the integration constant C with the natural constraint $|\sin(2\theta)| \leq 1$. The plane $(\varepsilon, \sin(2\theta))$ is the phase plane. Depending on the parameter ratios $(\gamma/e, \sigma/e)$ one can determine the regions in the phase space where the vortex stretching into filaments is possible and, vice versa, the regions having no such stretching. Since the parameter K does not change during the vortex strain by the barotropic flow, it is convenient to study the character of the vortex behavior on the plane of the dimensionless parameters $(\sigma/e, \gamma/e)$ for fixed K [21–23].

The condition $|\gamma/e| \leq 1$, which is imposed on the background current, is the necessary but not sufficient condition of unlimited stretching of the vortex. Let us call the above inequality the condition of possible stretching of the vortex. On the plane $(\sigma/e, \gamma/e)$, one can isolate several various regions depending on the parameter ratio (see Fig. 2). Three regions are distinguished along the vertical axis, for two regions where $|\gamma/e| > 1$, only oscillatory and rotational regimes (red color; the region extends to infinity) are present. In the region $|\gamma/e| \leq 1$, all the three regimes, which are separated by four curves exiting in pairs from the points $(0; \pm 1)$ and $(\pm\sigma/e, \pm 1)$, are permitted. As a result, the strip $|\gamma/e| \leq 1$ is divided into three zones, which are symmetric with respect to the origin of coordinates: the external zone (green color) in which all regimes are permitted (rotational, oscillatory, and stretching), the intermediate zone (yellow color) in which

4

the oscillatory regime and the regime of unlimited stretching are possible, and the internal zone (violet color) in which only the regime of unlimited stretching of the vortex core is permitted.

The regime of unlimited stretching of the vortex core is of the greatest interest to us (the violet zone in Fig. 2). In this case, there exists a limitation on the vortex intensity, i.e., the parameter $|\sigma/e|$ is limited. Conventionally, weak vortices correspond to this zone. Note that weak vortices are inevitably stretched into vortex filaments in the case of an additional requirement $|\gamma/e| \leq 1$. However, the notion of "weak vortices" should be treated with some caution, because the actual values of the parameter $|\sigma/e|$ can be great in this zone for small values of K. In this case, it is important to allow for the restrictions $|\gamma/e| \leq 1$ imposed on the background-current parameters, i.e., the strain properties of the currents should be stronger than their "rotational" properties

The analysis of different behavior of a vortex on the parameter plane $(\sigma/e, \gamma/e)$ has revealed an asymmetry of the zone corresponding to the regime of unlimited stretching of the vortex core (violet zone). The vortices satisfying the condition $\sigma/e < 0$ for $\gamma/e > 0$ and the condition $\sigma/e > 0$ for $\gamma/e < 0$, i.e., the vortices whose sign of the potential vorticity σ of the core is opposite to the sign of the conventional vorticity $\mathrm{rot}_z\mathbf{u}$ of the background current, are "better" subject to stretching. Vice versa, the vortices for which the signs of σ and $\mathrm{rot}_z\mathbf{u}$ coincide withstand stretching more "successfully."

Let us also emphasize an interesting property of the zone strain representing the regime of unlimited stretching of the vortices, namely, that the background currents with weak deformation properties are able to stretch a strong vortex. This fact can be explained by an analogy between the interaction of the background current with a vortex and the gravitational interaction of stars with interstellar dust. Mathematically, both problems are the same. If the integral mass of the dust exceeds the star mass, then the dust strongly affects the star motion despite the small density of the dust mass compared with the star density. In the case considered, the role of density is played by the potential vorticity and that of the gravitational potential, by the function of current. Consequently, if the integral vorticity of the current exceeds that of the vortex, then the effect of the current on the vortex is strong despite the strong difference in the potential vorticities of the above-mentioned hydrodynamic objects [21–23]. Analyzing Fig. 2, we should emphasize two other important conclusions. Only a very intense vortex with $\sigma/e < 0$ survives in an inhomogeneous current for $\gamma/e > 0$ (for $\sigma/e > 0$ and $\gamma/e > 0$, weak vortices survive easier), and weak currents with $\gamma/e > 0$, especially for γ/e values that are close to 1 but do not exceed it, are able to stretch a strong vortex into a filament with $\sigma/e < 0$.

The same is valid for weak currents with $\gamma/e < 0$ in the vicinity of the $\gamma/e \approx -1$ values (provided that $|\gamma/e| \leq 1$) and for intense vortices with $\sigma/e > 0$. Therefore, the following qualitative conclusion can be drawn: the fulfillment of the condition $|\gamma/e| \leq 1$ imposed on the background-current parameters is an important attribute of a possibility for vortices to stretch into a filament. In this case, the conventionally weak vortices are necessarily stretched, while the strong vortices are stretched depending on their parameters and the initial conditions.

Restrictions on the vortex intensity in the inevitable-stretching region (the violet zone in Fig. 2) allow one to conclude that a pronounced part of the ocean vortices fall within this zone according to their parameters, although the vortex stretching is forbidden in the water areas where $|\gamma/e| > 1$. Therefore, if we single out the regions on the world-ocean map with the condition $|\gamma/e| \leq 1$ imposed on the parameters of the background currents, one should expect in the latter a manifestation of the current properties to stretch the vortices into filaments in such regions and the number of stretching vortices should be sufficiently large.

3. ENERGY REDISTRIBUTION DURING VORTEX STRETCHING

Energy transformation during mesoscale-vortex stretching in the Norwegian Sea is considered in [24]. In the filament formed as a result of the vortex stretching, the longitudinal scale was more than 4 times higher than the transverse one. The stretching process was accompanied by a decrease in the vortex energy, i.e., the kinetic and potential energies decreased by a factor of 3 and 1.7, respectively. The total energy of the vortex decreased by a factor of 2.3. A comparison of theoretical and empirical calculations showed a fairly good quantitative correspondence of the results. Therefore, it has been found that the process of the

vortex transformation during its stretching is accompanied by the energy redistribution. Then one may ask where the energy lost by the vortex transfers to.

Let us single out two energy-redistribution mechanisms. The first mechanism involves the energy pumping from the circular-vortex scales to the transverse scale of the stretched vortices. This is a direct energy cascade of energy transfer from the mesoscale processes toward the submesoscale ones. When the vortex is stretched, the initial energy concentrated on its characteristic horizontal dimensions is redistributed to smaller scales of the order of the horizontal width of the filament. Such a mechanism is one of the possible ways to transfer energy from the mesoscale formations to the submesoscale ones. The second mechanism refers to the inverse energy cascade, when the energy lost by the stretched vortex returns to the background current due to the non-dissipativity of the vortex-current physical system. In the literature, this process is sometimes called a phenomenon with negative viscosity [25]. However, both mechanisms need additional studies.

4. A LAW OF CONSERVATION OF THE INTEGRAL AREAS OF THE DOMAINS WITH SOME PROPERTIES

The theory of evolution of the mesoscale vortices and a study of variants of their behavior have obtained a new impetus in the form of applications to actual ocean. The maps of the spatial distribution of the regions with different values of the parameters γ/e and σ/e are given in [21–23] for the entire World Ocean. A fraction of the domains in which the vortex stretching is permitted has been analyzed. The integral area of such domains is denoted as $S_{\leq 1}$. Further studies of the conservation of this value for the World Ocean with spatiotemporal averaging of the data have shown that the estimates remain fairly stable and satisfy the inequalities

$$1.5 < \frac{S_{\leq 1}}{S_{>1}} < 1.9, \tag{6}$$

$$0.60 < \frac{S_{\leq 1}}{S} < 0.67. \tag{7}$$

Here, $S_{>1}$ is the integral area of the domains where the unlimited stretching of vortices is forbidden and S is the total area of the considered water region. This result is rather unexpected. It is indicative of the existence of a certain "harmony" in the World Ocean, which was observed during the vortex interaction with currents. It turns out that regardless of the intensity of the currents, there exist a balance and some stability in the values of the integral areas of the domains in which the condition $|\gamma/e| > 1$ is fulfilled and, accordingly, the stretching of the vortices is prohibited and the domains with $|\gamma/e| \leq 1$, in which the regime of unlimited vortex stretching is permitted. Moreover, it is shown that this conclusion does not depend on the season and is confirmed by numerical estimates obtained for various years [23]. Thus, we can postulate the existence of another conservation law for the World Ocean (along with the laws of conservation of mass or potential vorticity), namely, the empirically obtained law of conservation of integral areas of domains with certain properties. Here we consider the ability of vortices to be stretched into filaments. It turns out that, in the World Ocean, the integral areas of domains with certain properties are consistent with each other (see the inequalities given in Eqs. (6) and (7)). However, this empirically obtained fact certainly needs theoretical justification today. Moreover, it turned out that the estimates of the integral areas of domains with certain properties, varying for the entire World Ocean, only slightly differ for individual water areas and also depend on the spatial averaging of the data. This issue is considered below for some water areas of the World Ocean.

5. THE DATA USED

The study has been performed using the data of the global oceanic reanalysis GLORYS12V1, which is available at Copernicus Marine Service (CMEMS) [26]. The data has a spatial resolution of 0.083° in latitude and longitude (the data with a discreteness of 1° was used in the work) and 50 levels vertically.
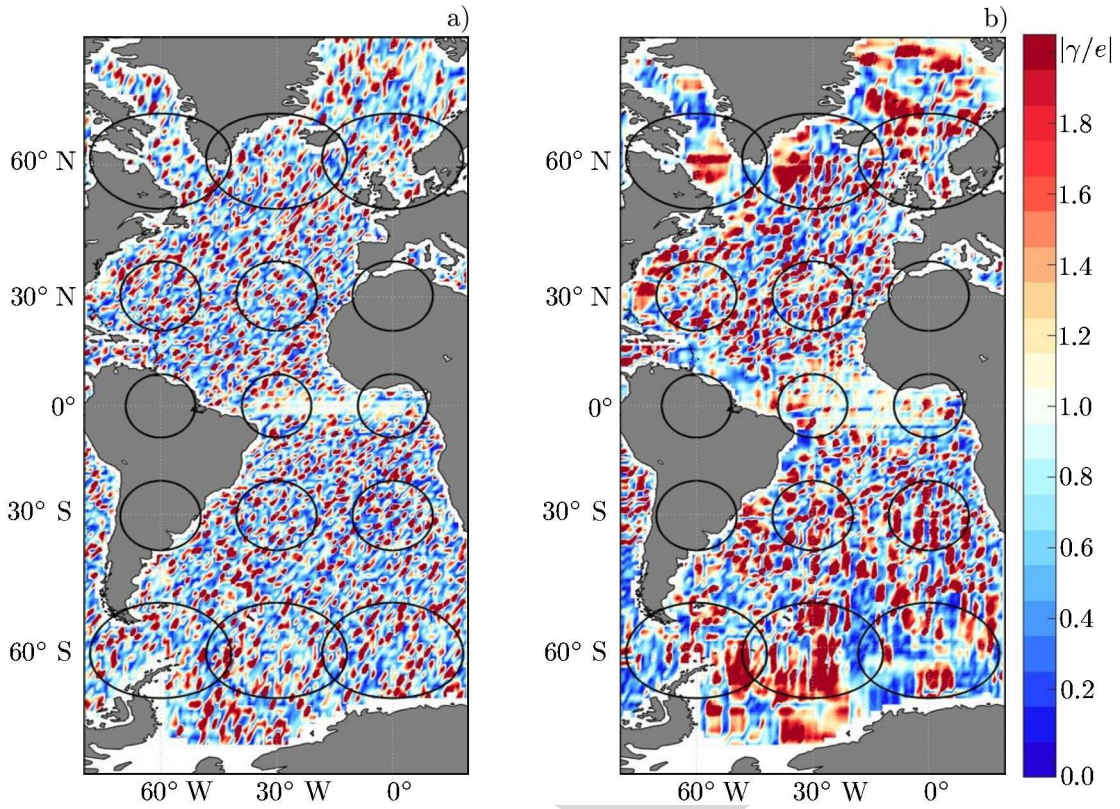
Fig. 3. Spatial distributions of domains in the Atlantic Ocean for June, 2010, which have been developed on the basis of the input data (a) and using by the moving-average method with the window width 10×10 cells (b). The ovals on the map correspond to the images of the circles on the globe with a radius of 1000 km. On the average, one can observe 9–11 "spots" on the ellipse-diameter line. Calculations using the equivalent circles for $30°$ N and $30°$ S have shown that the characteristic dimension of a "spot" is about 200 km (10 "spots" per 2000 km).

The GLORYS12V1 reanalysis assimilates the data along the tracks from the high-resolution altimeters, as well as the satellite observations of the sea-surface temperature, the sea-ice concentration, and the *in situ* temperature and salinity profiles. The reanalysis is based on the NEMO model in which the ECMWF ERA-Interim reanalysis is used as forcing. The data for the period 1993–2919 have been considered. The time resolution of the data is one day. All calculations were carried out for an average surface layer with a vertical thickness of 200 m.

6. USING THE ANALYSIS OF THE PHASE PORTRAIT ON THE PLANE ($\sigma/e, \gamma/e$) FOR INDIVIDUAL REGIONS

6.1. Atlantic Ocean

Figure 3 shows the distributions of γ/e for various variants of the spatial averaging. Let us estimate the areas occupied by the domains with certain properties. For the one-degree grid (Fig. 3a), the integral area of the domains with $|\gamma/e| > 1$ amounts to $3.29 \cdot 10^{13}$ m^2 (red color; the vortex stretching into filaments is prohibited) and the integral area of the domains with $|\gamma/e| \leq 1$ amounts to $5.88 \cdot 10^{13}$ m^2 (blue color; an unlimited stretching of the vortices is permitted). The ratio $S_{\leq 1}/S_{>1} \approx 1.78$, i.e., the fraction $S_{\leq 1}/S$ amounts to about 64%. For the smoothed data with the window width 10×10 cells (Fig. 3b), the integral area of the domains with $|\gamma/e| > 1$ amounts to $3.90 \cdot 10^{13}$ m^2, and the integral area of the domains with $|\gamma/e| \leq 1$ equals $5.27 \cdot 10^{13}$ m^2. The ratio $S_{\leq 1}/S_{>1} \sim 1.35$, i.e., the fraction $S_{\leq 1}/S$ amounts to about 57%.
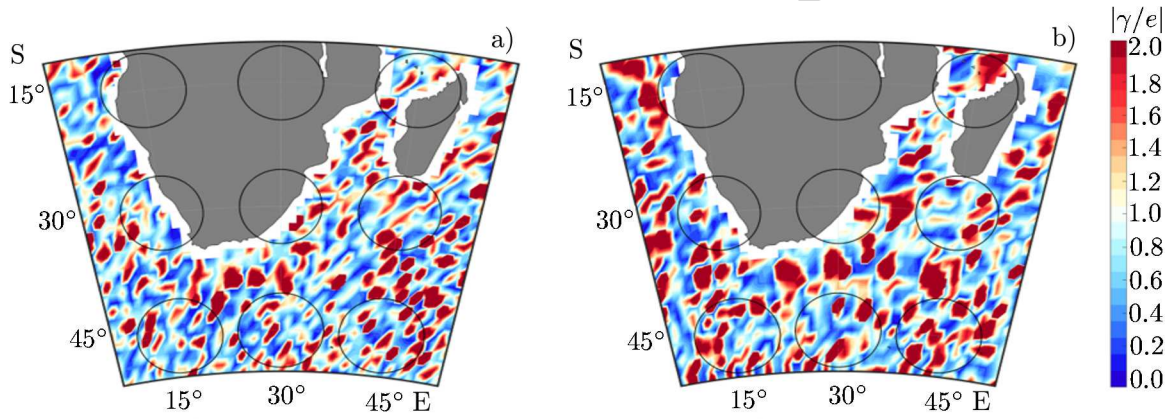
7

Fig. 4. The spatial distributions of the domains in the region of the Agulhas current for June, 2010, which have been developed on the basis of the input data (a) and using the moving-average method with the window width 5×5 cells (b). The circle radii amount to 500 km.

6.2. The Agulhas-current area

Figure 4 shows the distributions of γ/e for two variants of the spatial averaging. For the one-degree grid (Fig. 4a), the integral area of the domains with $|\gamma/e| > 1$ amounts to $5.48 \cdot 10^{12}$ m^2 and the integral area of the domains with $|\gamma/e| \leq 1$ equals $9.27 \cdot 10^{12}$ m^2. The ratio $S_{\leq 1}/S_{>1} \approx 1.69$, i.e., the fraction $S_{\leq 1}/S$ amounts to about 63%. For the smoothed data with the window width 5×5 cells (Fig. 4b), the integral area of the domains with $|\gamma/e| > 1$ amounts to $5.89 \cdot 10^{12}$ m^2, while the integral area of the domains with $|\gamma/e| \leq 1$ equals $8.87 \cdot 10^{12}$ m^2. The ratio $S_{\leq 1}/S_{>1} \approx 1.51$, i.e., the fraction $S_{\leq 1}/S$ is equal to about 60%. Since the diameter of the circles is 1000 km and about 5 domains are located inside each circle, the estimated scales of the domains are about 200 km.

6.3. The Weddell Sea

Let us consider the temporal variability of the location of domains using an example of a water area located in the Weddell Sea according to the data for 2010. Figure 5 shows that the domain distributions are different for various days. Accordingly, the integral area of the domains of a certain property in this water area also changes. Indeed, according to Fig. 6, $3.62 \cdot 10^{12}$ m$^2 < S_{\leq 1} < 4.27 \cdot 10^{12}$ m^2. The inequality $0.55 < S_{\leq 1}/S < 0.64$ is also satisfied. The obtained estimates differ from those in Eq. (7), which means that regionally the law of conservation of the integral areas of the domains with certain properties has some features and the estimates can differ for various regions. It should also be emphasized that, as before, the integral areas of the domains having the property of the vortex stretching exceed the total areas of domains with the opposite property.

Therefore, the distribution of the domains with certain properties and the estimates of their integral areas differ for various regions of the World Ocean and also depend on the averaging. Figure 7 shows the hystograms of the current distributions of $|\gamma/e|$ for the period 1993–2019, which were calculated from the initial one-degree data and the data smoothed by the moving average with the window 10×10 cells. Obviously, irrespective of the averaging, the major part of the values satisfies inequality $|\gamma/e| \leq 1$. Therefore, the vortex ability of stretching when interacting with the background currents is a fundamental property of the mesoscale vortices in the ocean.

7. CONCLUSIONS

On the parameter plane $(\sigma/e, \gamma/e)$, we have analyzed the behavior regimes of the vortices in the ocean during their interaction with the background current. The zones with permitted and prohibited unlimited stretching of the vortices have been isolated for various water areas of the World Ocean.
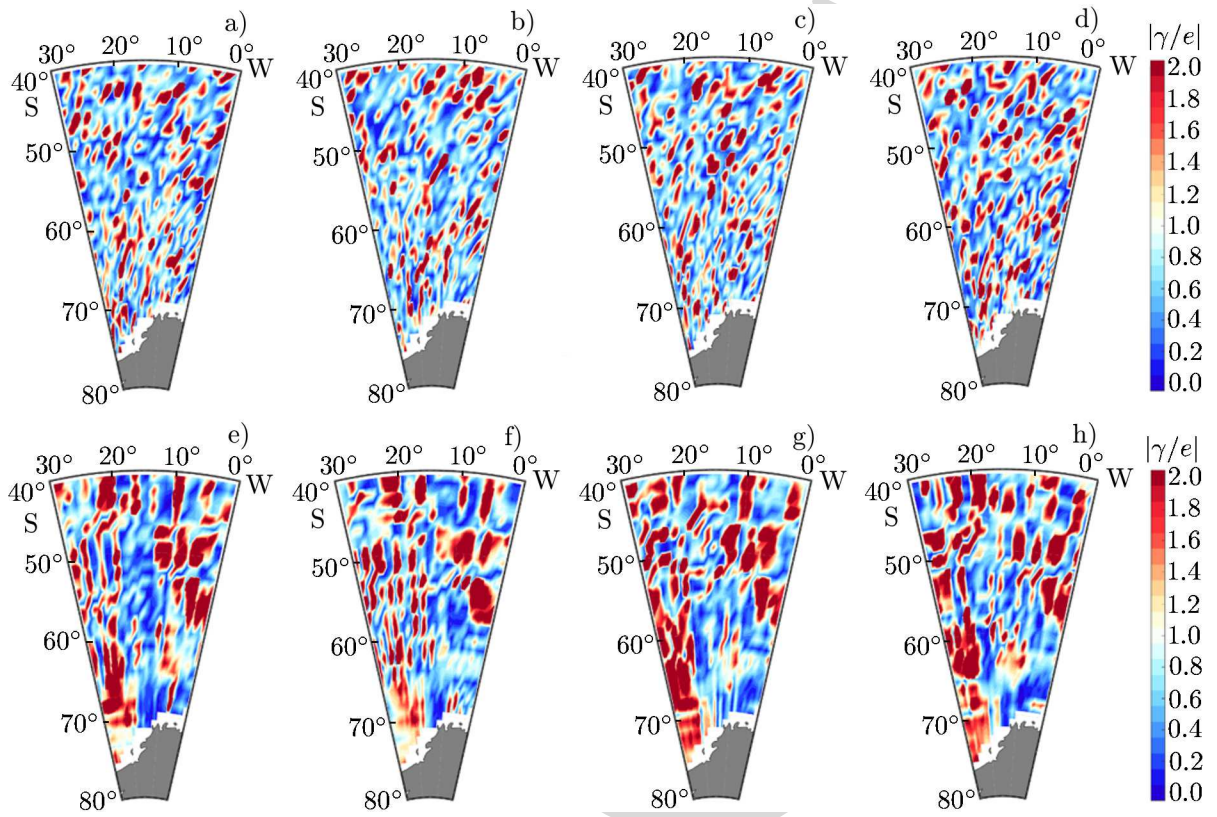
8

Fig. 5. Spatial distribution of the domains in the Weddell Sea on January 1, 2010 (a), April 1, 2010 (b), July 1, 2010 (c), and October 1, 2010 (d). Panels a–d have been developed based on the input data, while panels e–h, on the data smoothed by the moving average with the window 10×10 cells.
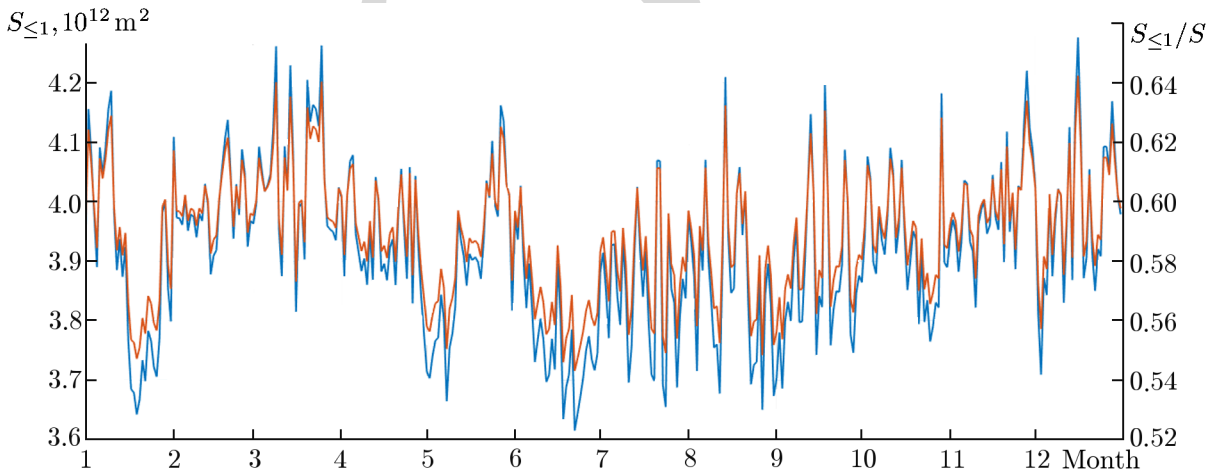

Fig. 6. Seasonal trend of variability of the integral area $S_{\leq 1}$ of the domains with the property $|\gamma/e| \leq 1$ (blue curve) and $S_{\leq 1}/S$ (orange curve) in the Weddell Sea for 2010.

It has been shown that the vortex stretching into vortex filaments on the ocean surface is manifested in the form of domains whose share of the considered water area amounts to 55–64%. The characteristic dimensions of the spots amount to about 200 km. The vortex stretching into the vortex filaments ensures the energy "pumping" from mesoscale processes to submesoscale ones.

On the basis of the data of the global oceanic reanalysis GLORYS12V1, we have developed the distributions of the domains with various properties, which characterize the regimes of unlimited stretching
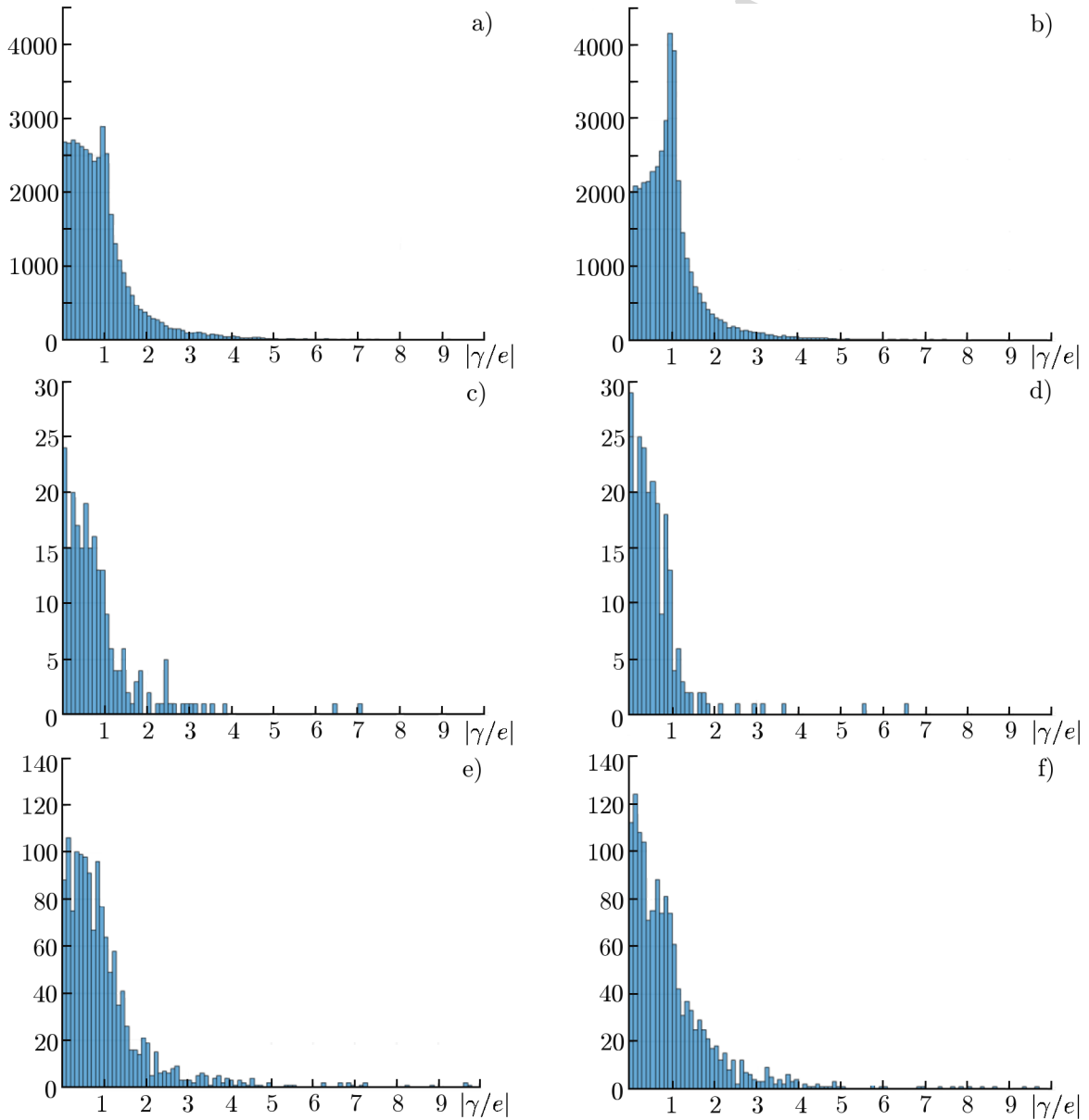
9

Fig. 7. Histograms of the distributions of $|\gamma/e|$ for the one-degree grid (a, c, and e) and the data of averaging with the window 10×10 cells (b, d, and f) for the period 1993–2019 for the World Ocean (a and b), the Lofoten Basin (c and d), and the Agulhas current (e and f).

of the mesoscale vortices into submesoscale filaments under the action of the barotropic current. All the calculations have been carried out for an averaged surface layer with a vertical thickness of 200 m. It has been shown that the integral surface area of the considered water regions (the Atlantic Ocean, the Agulhas-current region, and the Weddell Sea) with the vortex property of unlimited stretching exceeds the integral area of the regions with prohibited stretching.

Having analyzed the monthly averaged data of GLORYS12V1 for 1993–2019, we have shown that the share of the integral regions of the world-ocean surface, where the vortices can stretch when interacting with the barotropic current amounts to about 60% and neither interannual nor seasonal variability are present for this estimate. In the case of the spatial averaging of the data, the domain scales increase, but the shares of the domains with different properties vary only slightly and, on the whole, satisfy Eqs. (6) and (7). This property is fulfilled for both the surface of the entire World Ocean [23] and individual water areas (the Atlantic Ocean, the Agulhas-current region, and the Weddell Sea). The current-distribution hystograms, which were plotted

for the period 1993–2019 for both a one-degree grid and the data of averaging with the width 10×10 cells by the moving-average method, have shown that irrespective of the averaging, the major part of the World Ocean area corresponds to the parameter values $|\gamma/e| \leq 1$. This, in turn, means that one should expect the vortex stretching into filaments on the overwhelming part of the sea territory (55–64%). The inverse energy cascade should be manifested in the same zones, which is equivalent to the negative-viscosity property.

The obtained results should be allowed for when developing hydrodynamic models of the World Ocean.

APPENDIX

7.1. The elements of the theory of ellipsoidal vortices

For the presentation integrity, we briefly delineate a theoretical approach to an analytical description of the vortices with an ellipsoidal core shape. A detailed description of the theory can be found in [8, 14]. The use of this theory is given, in e.g., [21–23, 27] for various variants.

Let us consider an ocean with constant Brunt–Väisälä frequency. The Rossby number is assumed to be small. It is also assumed that the vortex core is an arbitrarily-shaped freely deformable "water bag" filled with a liquid having a uniform potential vorticity σ of liquid particles, outside of which the potential vorticity is equal to zero. Let the quasigeostrophic approximation be valid. In this formulation, the mathematical problem is reduced to solving the nonlinear nonstationary equation for the pressure or the current function. The above-mentioned equation is reduced to the dimensional form in terms of the current function $\psi(x, y, z, t)$:

$$\frac{\partial}{\partial t}\left(\Delta_{\mathrm{h}}\psi + \frac{\partial}{\partial z}\frac{f^2}{N^2}\frac{\partial \psi}{\partial z}\right) + J_{\mathrm{h}}\left(\psi, \Delta_{\mathrm{h}}\psi + \frac{\partial}{\partial z}\frac{f^2}{N^2}\frac{\partial \psi}{\partial z}\right) = 0. \tag{A1}$$

Here, x and y are the fixed horizontal axes of the coordinate system, z is the vertical axis, $J_{\mathrm{h}}(A, B) = (\partial A/\partial x)(\partial B/\partial y) - (\partial A/\partial y)(\partial B/\partial x)$ is the Jacobian, Δ_{h} is the Laplace operator with respect to the horizontal coordinates x and y, f is the Coriolis parameter, and N is the Brunt–Väisälä frequency. If the current function $\psi(x, y, z, t)$ is found, all the remaining hydrodynamic characteristics of motion, e.g., the velocity field (u, v, w), can be calculated:

$$u = -\frac{\partial \psi}{\partial y}, \qquad v = \frac{\partial \psi}{\partial x}, \qquad w = -\frac{f_0}{N^2}\left[\frac{\partial^2 \psi}{\partial t\,\partial z} + J_{\mathrm{h}}\left(\psi, \frac{\partial \psi}{\partial z}\right)\right]. \tag{A2}$$

The physical meaning of Eq. (A1) is in preserving the potential vorticity σ of a moving liquid particle:

$$\sigma = \Delta_h\psi + \frac{\partial}{\partial z}\frac{f^2}{N^2}\frac{\partial \psi}{\partial z}. \tag{A3}$$

In this case, $\mathrm{rot}_z\mathbf{u} = \Delta_{\mathrm{h}}\psi$. If it is assumed that the ocean is unlimited in all directions, the Brunt–Väisälä frequency is constant ($N = \mathrm{const}$), the liquid rests at infinity, the deformable core of the vortex with a liquid boundary is an arbitrarily shaped simply connected volume, and all the vortex-core particles have the same potential vorticity σ, then, instead of the basic nonlinear equation (A1), one can solve an equivalent linear problem of seeking the current function for the stepwise distribution of σ in the space $(x, y, \tilde{z})$:

$$\Delta\psi = \begin{cases} \sigma, & \text{if the point is inside the core;} \\ 0, & \text{if the point is outside the core.} \end{cases} \tag{A4}$$

Here, $\tilde{z} = (N/f)z$ is the stretched vertical coordinate. Problem (A4) is equivalent to that of the gravitational

potential and is solved in the general form for an arbitrary shape V of the core in the "stretched" coordinates $(x, y, \tilde{z})$;

$$\psi(x, y, \tilde{z}) = -\frac{\sigma}{4\pi} \int \int\limits_{V} \int \frac{\mathrm{d}x'\, \mathrm{d}y'\, \mathrm{d}\tilde{z}'}{\sqrt{(x - x')^2 + (y - y')^2 + (\tilde{z} - \tilde{z}')^2}}. \tag{A5}$$

The current function ψ in Eq. (A5) is continuous in the entire space along with the first derivatives. Since the continuity of ψ is equivalent to the pressure continuity, the pressure is the same on both sides of the core boundary, which automatically satisfies the dynamic boundary condition on the vortex-core surface. Differentiating the current function $\psi(x, y, \tilde{z})$ with respect to x and y under the integral sign, one can calculate the horizontal components of the induced velocities, which also turn out to be continuous.

As a result, Eq. (A5) is a solution of problem (A1) with the satisfied dynamic condition on the core boundary at a certain fixed time instant when the core shape V is specified.

Integral (A5) changes with varying core shape. The time is contained as a parameter in the core shape V. However, solution (A5) should be subject to another restriction, i.e., the kinematic boundary condition should be fulfilled on the core surface. If we denote $F(x, y, \tilde{z}, t) = 0$ as an equation of the core boundary, the kinematic condition takes the form

$$\frac{\partial F}{\partial t} + u\frac{\partial F}{\partial x} + v\frac{\partial F}{\partial y} + w\frac{\partial F}{\partial z} = 0. \tag{A6}$$

For small Rossby numbers, the last term should be neglected and the kinematic condition is simplified to

$$\frac{\partial F}{\partial t} + u\frac{\partial F}{\partial x} + v\frac{\partial F}{\partial y} = 0, \tag{A7}$$

where

$$u(x, y, \tilde{z}, t) = -\frac{\sigma}{4\pi} \iiint\limits_{V} \frac{(y - y')\, \mathrm{d}x'\, \mathrm{d}y'\, \mathrm{d}\tilde{z}'}{[(x - x')^2 + (y - y')^2 + (\tilde{z} - \tilde{z}')^2]^{3/2}}, \tag{A8}$$

$$v(x, y, \tilde{z}, t) = \frac{\sigma}{4\pi} \iiint\limits_{V} \frac{(x - x')\, \mathrm{d}x'\, \mathrm{d}y'\, \mathrm{d}\tilde{z}'}{[(x - x')^2 + (y - y')^2 + (\tilde{z} - \tilde{z}')^2]^{3/2}}. \tag{A9}$$

Recall that the function $F(x, y, \tilde{z}, t)$ is the boundary of the region V and, therefore, Eq. (A6) with the velocities values (A8) and (A9) is the integro-differential equation for describing the core-shape evolution. Its numerical implementation is the basis for the method of the contour dynamics in the two-dimensional hydrodynamics and the method of the surface dynamics for 3D vortices.

The described approach to considering the vortex evolution can be used for solving a more general problem of vortex evolution against the background of the current. The current should also have a constant potential vorticity. Such a modification is possible for constant-vorticity currents, in particular, for barotropic flows, which are linear with respect to the horizontal coordinates. In this case, the kinematic condition (A7) becomes somewhat changed:

$$\frac{\partial F}{\partial t} + (u + u_{\mathrm{b}})\frac{\partial F}{\partial x} + (v + v_{\mathrm{b}})\frac{\partial F}{\partial y} = 0. \tag{A10}$$

Here, $(u_{\mathrm{b}}, v_{\mathrm{b}})$ are the specified horizontal components of the background current, (u, v) is the eigenfield of the currents from the vortex, $F(x, y, \tilde{z}, t) = 0$ is still the core-boundary equation, and the parameter σ in Eqs. (A5), (A8), and (A9) is the redundant potential vorticity of the vortex core compared with the potential vorticity of the background current. The integro-differential equation remains valid.

The analytical solution of Eqs. (A7) and (A10) is possible if the integrals in Eqs. (A5), (A8), and (A9) are evaluated in closed form. Exactly this situation is realized if the vortex-core shape is specified in the form of an ellipsoid which preserves the ellipsoidal shape during its self-strain and the strain by the background current. These conditions are fulfilled if the background current is linear with respect to the coordinates.

12

These properties are typical of the constant-vorticity barotropic current. In this case, the integro-differential equation into a differential equation, which, in turn, is transformed to a set of ordinary differential equations for the ellipsoid parameters, i.e., the lengths of its semiaxes and the angle of rotation around the vertical axis.

Below, we show the solution $\psi(\tilde{x}, \tilde{y}, \tilde{z}, t)$ of problem (A5) for an ellipsoid and also write the horizontal components of the vortex-induced velocities (u_v, v_v):

$$\psi(\tilde{x}, \tilde{y}, \tilde{z}, t) = -\frac{1}{4}\sigma ab\tilde{c} \int\limits_{\lambda}^{\infty} \left(1 - \frac{\tilde{x}^2}{a^2 + \mu} - \frac{\tilde{y}^2}{b^2 + \mu} - \frac{\tilde{z}^2}{\tilde{c}^2 + \mu}\right) \frac{\mathrm{d}\mu}{\sqrt{(a^2 + \mu)(b^2 + \mu)(\tilde{c}^2 + \mu)}},$$

$$u_v = -\frac{\sigma}{2}ab\tilde{c} \int\limits_{\lambda}^{\infty} \frac{\mathrm{d}\mu}{(b^2 + \mu)\sqrt{(a^2 + \mu)(b^2 + \mu)(\tilde{c}^2 + \mu)}}\tilde{y},$$

$$v_v = \frac{\sigma}{2}ab\tilde{c} \int\limits_{\lambda}^{\infty} \frac{\mathrm{d}\mu}{(a^2 + \mu)\sqrt{(a^2 + \mu)(b^2 + \mu)(\tilde{c}^2 + \mu)}}\tilde{x}. \tag{A11}$$

Here, a and b are the horizontal semiaxes of the ellipsoid, c is its vertical semiaxis, $\tilde{c} = (N/f)c$ is the vertical semiaxis stretched by a factor of N/f, $\tilde{x}$ and $\tilde{y}$ are the horizontal coordinate axes directed along the main ellipsoid axes, and $\tilde{z} = (N/f)z$ is the stretched (by a factor of N/f) vertical axis of the coordinate system. The semiaxes a and b can depend on both the time and the parameter. The lower limit $\lambda(\tilde{x}, \tilde{y}, \tilde{z})$ in integral (A11) is a positive root of the cubic equation

$$\frac{\tilde{x}^2}{a^2 + \lambda} + \frac{\tilde{y}^2}{b^2 + \lambda} + \frac{\eta^2}{\tilde{c}^2 + \lambda} = 1. \tag{A12}$$

We should put $\lambda = 0$ inside the core up to its boundary. Let us note that the current function at the boundary of the ellipsoidal core is quadratic with respect to the coordinates, while the velocity is linear. In the ocean resting at infinity, the vortex core rotates around the vertical axis without the shape deformation. The particles inside the core move faster than the core-shape rotation. The details can be found in [8, 14]. Note that solution (A11) is an exact solution of the initial nonlinear nonstationary problem (A1).

As was noted above, if such an ocean with the vortex is superimposed by a background constant-vorticity barotropic current, which is linear with respect to the horizontal coordinates, such that

$$u_{\mathrm{b}} = u_0 + ex - \gamma y; \qquad v_{\mathrm{b}} = v_0 + \gamma x - ey, \tag{A13}$$

then an approach developed above for the resting ocean can also be used in this case. The background-current characteristics are as follows. The parameter $\gamma = (1/2)|\mathrm{rot}_h\mathbf{U}_{\mathrm{b}}|$ is the angular rotation velocity of the background current (A13), where $\mathbf{U}_{\mathrm{b}} = (u_{\mathrm{b}}, v_{\mathrm{b}})$. Since the strain-rate tensor $\begin{pmatrix} e & 0 \\ 0 & -e \end{pmatrix}$ of the current (A13) depends only on the parameter e, the presence of $e \neq 0$ in the background current (A13) supplies it with a property to strain liquid objects. The system of horizontal coordinates (x, y), in which the velocity (A13) is written, is motionless. Note that the coordinate systems $(x, y, \tilde{z})$ and $(\tilde{x}, \tilde{y}, \tilde{z})$ are different but have the common axis $\tilde{z}$.

The linear dependence of the background-current velocity on the coordinates in the theory of ellipsoidal vortices is of fundamental importance. As the coordinate system is rotated around the vertical axis, the linear dependence on the coordinates is retained but the coefficients change. With any linear dependence of the background-current field on the horizontal coordinates, it is always possible to choose such a rotation of the coordinate system that the velocity distribution (A13) is realized in the new system. The background current (A13) $\mathbf{U}_{\mathrm{b}} = (u_{\mathrm{b}}, v_{\mathrm{b}}, 0)$ is the most general form of the barotropic current which is linear with

13

respect to the horizontal coordinates. Both the potential and usual vorticity are constant in this current and coincide with the curl $\mathrm{rot}_z\mathbf{u}_\mathrm{b} = 2\gamma$ of the background-current velocity. The velocity distribution (A13) can be represented as an expansion of a large-scale barotropic current into a Taylor series in the vortex vicinity if we confine ourselves to terms which are linear with respect to the coordinates.

Solution (A11) in the above-mentioned current (A13) still holds and the vortex core still has ellipsoidal shape, but the parameter σ in Eq. (A11) should be interpreted as a redundant potential core vorticity above its background value. In other words, the potential vorticity for the core particles is uniform and equals $2\gamma + \sigma$ and the potential vorticity for the liquid particles which are external with respect to the core is also constant and equals 2γ. The core behavior in the current also changes. First of all, the core moves with a velocity of the external background current with a translational velocity $(u_0, v_0, 0)$ of the core center and its strain is described by the following system of equations for the evolution of the horizontal semiaxes $a(t)$ and $b(t)$ and the rotation angle θ of the major semiaxis with respect to the x-axis direction:

$$\dot{a} = eb\cos(2\theta); \tag{A14}$$

$$\dot{b} = -ea\cos(2\theta); \tag{A15}$$

$$\dot{\theta} = \Omega(a, b, \tilde{c}) + \gamma - \frac{a^2 + b^2}{a^2 - b^2}e\sin(2\theta). \tag{A16}$$

Here, $\Omega(a, b, \tilde{c})$ is the natural angular velocity of the vortex-core rotation around the vertical axis. The expression for $\Omega(a, b, \tilde{c})$ is given below in more convenient variables. Obviously, in the general case, the core is strained by the background current owing to the strain coefficient e in Eqs. (A14) and (A15) and rotates by analogy with the Kirchhoff-vortex rotation with the only difference in the term $\Omega(a, b, \tilde{c})$, still remaining ellipsoidal.

The horizontal semiaxes $a(t)$ and $b(t)$ vary over time with the preservation of the product $a(t)b(t) = \mathrm{const}$, while the vertical semiaxis c and, correspondingly, the stretched vertical semiaxis $\tilde{c} = (N/f)c$ remain intact. The integral $a(t)b(t) = \mathrm{const}$ allows us to reduce the order of the system of equations. (A14)–(A16) and pass to a new variable, i.e., the horizontal stretching $\varepsilon = a/b \geq 1$ of the vortex (here, the semiaxis a is the major one of among the horizontal semiaxes a and b).

After reducing the order, a new system of equations of the vortex-parameter evolution is given below as

$$\dot{\varepsilon} = e\varepsilon\cos(2\theta), \tag{A17}$$

$$\dot{\theta} = \Omega(\varepsilon, K) + \gamma - \frac{\varepsilon^2 + 1}{\varepsilon^2 - 1}e\sin(2\theta). \tag{A18}$$

Here, the natural angular velocity $\Omega(\varepsilon, K)$ of the vortex-core rotation is written in the dimensionless variables (ε, K), and $K = (N/f)\left(c/\sqrt{ab}\right)$ is the parameter of the vertical oblation of the core:

$$\Omega(\varepsilon, K) = \frac{1}{2}\sigma K \int\limits_0^\infty \frac{\mu\,d\mu}{\left[(\mu^2 + \mu + 1)^3(K^2 + \mu)\right]^{1/2}}. \tag{A19}$$

According to [8, 14], three behavior regimes can be singled out in the ellipsoidal-core evolution. Two of them, namely, the core-rotation and the core-oscillation regimes, are periodic. In the rotation regime, the long horizontal semiaxis of the core (the a semiaxis) undergoes a complete rotation by 360° for the period. In the oscillation regime, the long semiaxis periodically oscillates near a certain direction. In this case, a periodic limited variation in the lengths of the horizontal semiaxes is observed in both regimes. In the core-oscillation regime, liquid particles in the core continue rotating in the same direction, irrespective of the shape-oscillation phase.

The behavior of the vortex core in the unlimited-stretching regime is radically different. In this regime, the core does not have time to make even one complete revolution, but after the initial evolution stage, one

14

of the horizontal axes of the ellipsoid is infinitely stretched, while the second horizontal axis is reduced to zero. As before, the vertical axis, does not change.

The vortex formations which are relatively weak in terms of intensity, as well as the vortices which have already been sufficiently stretched in the horizontal direction from the very beginning of the evolution, are subject to the unlimited stretching regime. The inequality $|e| \geq |\gamma|$, which is imposed on the parameters of the background current (A13), is a necessary but insufficient condition for implementing the regime of the unlimited stretching of the vortex cores. If the inequality $|\gamma/e| \leq 1$ is valid in some region of the World Ocean, an unlimited stretching of the cores is permitted in that region. Otherwise, the stretching is prohibited for $|\gamma/e| > 1$. In the zones (domains) with a permitted unlimited stretching of the cores, part of the available vortices will stretch to filaments. First of all, they are weak vortices and sufficiently stretched ones. The share of the stretching vortices is still to be determined. This work has been aimed at finding the zones of the permitted stretching of the vortices in the World Ocean and at studying the simplest properties of these zones, i.e., their integral share in terms of the occupied area and variability of all their characteristics and dimensions.

REFERENCES

1. A. S. Monin and G. M. Zhikharev, *Sov. Phys. Usp.*, **33**, No. 6, 313–339 (1990). https://doi.org/10.1070/PU1990v033n05ABEH002569
2. O. Yu. Lavrova, A. G. Kostyanov, S. A. Lebedev, et al., *Complex Satellite Monitoring of Russia's Seas* [in Russian], Space Research Inst., Moscow (2011).
3. L. L. Fu and P.-Y. Le Traon, *Compt. Rend. Geosci.*, **338**, Nos. 14–15, 1063–1076 (2006). https://doi.org/10.1016/j.crte.2006.05.015
4. "International altimetry team," *Adv. Space Res.*, **68**, No. 2, 319–363 (2021). https://doi.org/10.1016/j.asr.2021.01.022
5. D. B. Chelton, M. G. Schlax, and R. M. Samelson, *Prog. Oceanogr.*, **91**, No. 2, 167–216 (2011). https://doi.org/10.1016/j.pocean.2011.01.002
6. S. A. Chaplygin, *Collected Works, Vol. 2* [in Russian], Gostekhizdat, Moscow (1948).
7. S. Kida, *J. Phys. Soc. Jpn.*, **50**, No. 10, 3517–3520 (1981).
8. V. V. Zhmur and K. K. Pankratov, *Okeanologiya*, **29**, No. 2, 205–211 (1989).
9. V. V. Zhmur and K. K. Pankratov, *Izv. Akad. Nauk. SSSR*, **26**, No. 9, 972–981 (1990).
10. V. V. Zhmur and A. F. Shchepetkin, *Izv. RAN, Fiz. Atmos. Oceana*, **27**, No. 5, 492–503 (1991).
11. V. V. Zhmur and K. K. Pankratov, *Phys. Fluids A: Fluid Dyn.*, **3**, No. 5, 1464–1464 (1991). https://doi.org/10.1063/1.857998
12. S. P. Meacham, *Dyn. Atmos. Oceans*, **16**, Nos. 3–4, 189–223 (1992). https://doi.org/10.1016/0377-0265(92)90007-G
13. S. P. Meacham, K. K. Pankratov, A. F. Shchepetkin, and V. V. Zhmur, *Dyn. Atmos. Oceans*, **21**, Nos. 2–3, 167–212 (1994). https://doi.org/10.1016/0377-0265(94)90008-6
14. V. V. Zhmur, *Mesoscale Vortices in the Ocean* [in Russian], GEOS, Moscow (2011).
15. V. V. Zhmur, E. V. Novoselova, and T. V. Belonenko, *Izv. Atmos. Oceanic Phys.*, **57**, No. 6, 632–641 (2021). https://doi.org/10.1134/S0002351521050151/1433821050157
16. V. V. Zhmur, E. V. Novoselova, and T. V. Belonenko, *Oceanology*, **61**, No. 6, 830–838 (2021). https://doi.org/10.1134/S0001437021060333
17. V. V. Zhmur, E. V. Novoselova, and T. V. Belonenko, *Oceanology*, **62**, No. 3, 289–302 (2022). https://doi.org/10.1134/S00014370222030171
18. K. V. Koshel, E. A. Ryzhov, and V. V. Zhmur, *Nonlin. Proc. Geophys.*, **20**, No. 4, 437–444 (2013). https://doi.org/10.5194/npg-20-437-2013
19. K. V. Koshel, E. A. Ryzhov, and V. V. Zhmur, *Phys. Rev. E*, **92**, No. 5, 053021 (2015). https://doi.org/10.1103/PhysRevE.92.053021

20. K. V. Koshel, E. A. Ryzhov, and V. V. Zhmur, *J. Marine Res.*, **69**, Nos. 2–3, 435–461 (2011). https://doi.org/10.1357/002224011798765204

21. V. V. Zhmur, T. V. Belonenko, E. V. Novoselova, and B. P. Suetin, *Dokl. Ros. Acad. Nauk. Nauki Zeml.*, **508**, No. 2, 270–274 (2023). https://doi.org/10.31857/S2686739722602113

22. V. V. Zhmur, T. V. Belonenko, E. V. Novoselova, and B. P. Suetin, *Oceanology*, **63**, No. 2, 174–183 (2023). https://doi.org/. org./10.1134/S0001437023020145

23. V. V. Zhmur, T. V. Belonenko, E. V. Novoselova, and B. P. Suetin, *Oceanology*, **63**, No. 2, 211–223 (2023). https://doi.org/10.31857/S0030157

24. V. V. Zhmur, V. S. Travkin, T. V. Belonenko, and D. A. Harutyunyan, *Mor. Gidrofiz. Zh.*, **38**, No. 5, 466–480 (2022).

25. V. P. Starr, *Physics of Negative Viscosity Phenomena*, McGraw-Hill, New York (1968).

26. https://data.marine.copernicus.eu/product/GLOBAL_MULTIYEAR_PHY_001_030/description

27. V. V. Zhmur and D. A. Harutyunyan, *Oceanology*, **63**, No. 1, 1–16 (2023). https://doi.org/10.1134/S0001437023010186